Turbulence & Diffusion in Canopies

- Small roughness elements create friction and pressure drag.
- When the turbulence created by the roughness elements becomes comparable to the turbulence in the flow, we have to treat the roughness elements as a separate canopy with its own internal flows.

Obstacles in the lower 100 m of the atmosphere distort the flow forming canopy layers. Vertically distributed sinks and sources result in a local modification of climate conditions. From: https://www.cliccs.uni-hamburg.de/research/theme-a/a3.html

Length and Time Scales

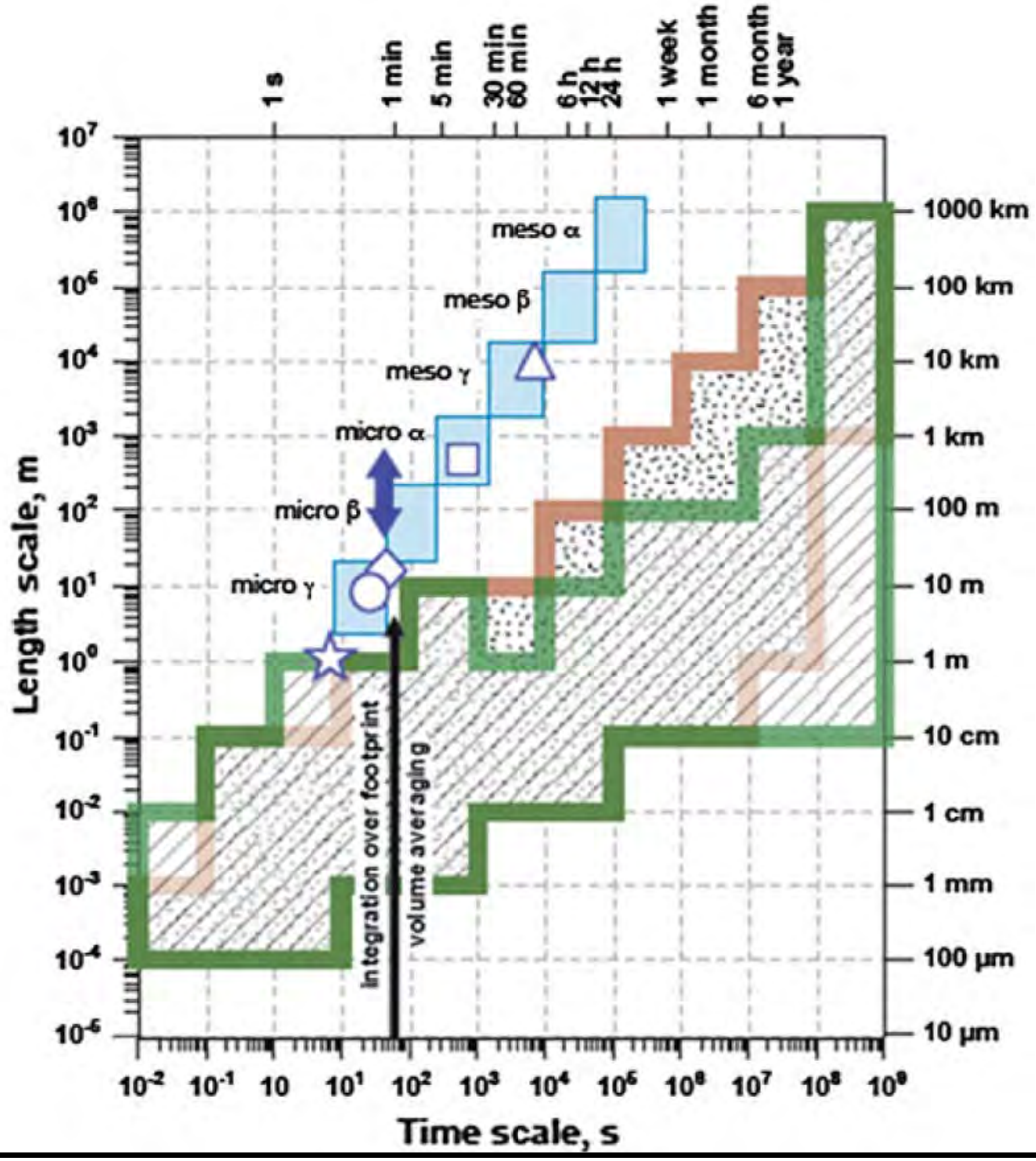

Fig. B1. Temporal and spatial scales of atmospheric (turbulent), plant (physiological), and soil processes. Atmospheric processes are given in light blue squares of one order of magnitude (from micro c to meso a). Forest canopy related transport processes comprise turbulent transport in canopy (white star), vertical advection in canopy (white circle), transport above canopy (white diamond), coherent structures (blue double arrow), footprint averaged turbulent flux (white square), and horizontal advection at canopy top (white triangle). The scales of plant processes, relevant for energy and matter exchange with the atmosphere are green. Those of soil processes are brown.

Foken et al., 2012, *ACP,* Vol 12.

Roughness and Displacement Height

Zero-Plane Displacement accounts for momentum lost in the canopy.

Smooth flow:

$$u(z) = \frac{u_*}{\kappa} \ln\left(\frac{z}{z_0}\right)$$

Modified to:

$$u(z) = \frac{u_*}{\kappa} \ln\left(\frac{z-d}{z_0}\right)$$

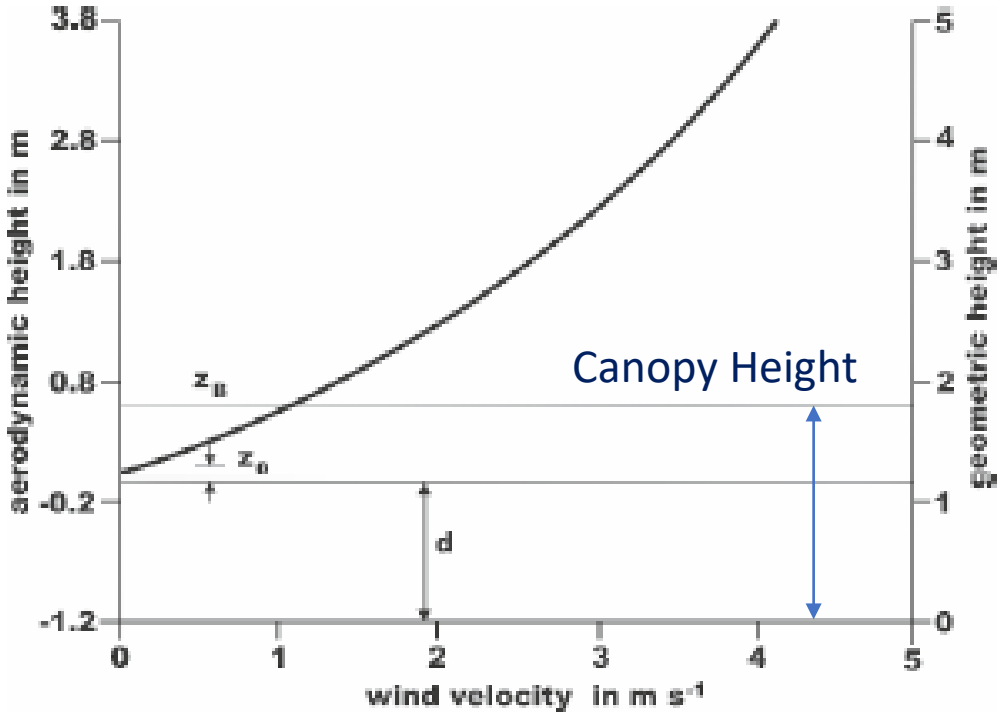

Similar for θ and q, without the bluff-body effect.

Foken, Ch 3. Kaimal & Finnigan, Ch 3

Flow above the Canopy

The Roughness Sublayer height (z_*).

$$\overline{u'w'} = -\frac{\kappa z}{\phi_*\left(\frac{z}{z_*}\right)\phi_m\left(\frac{z}{L}\right)}\frac{du}{dz}$$

$$\overline{w'T'} = -\frac{\alpha_0 \kappa z}{\phi_*\left(\frac{z}{z_*}\right)\phi_H\left(\frac{z}{L}\right)}\frac{dT}{dz}$$

$$\overline{w'q'} = -\frac{\alpha_{0E} \kappa z}{\phi_*\left(\frac{z}{z_*}\right)\phi_E\left(\frac{z}{L}\right)}\frac{dq}{dz}$$

$$\phi_*\left(\frac{z}{z_*}\right) = \exp\left[-0.7\left(1-\frac{z}{z_*}\right)\right]$$

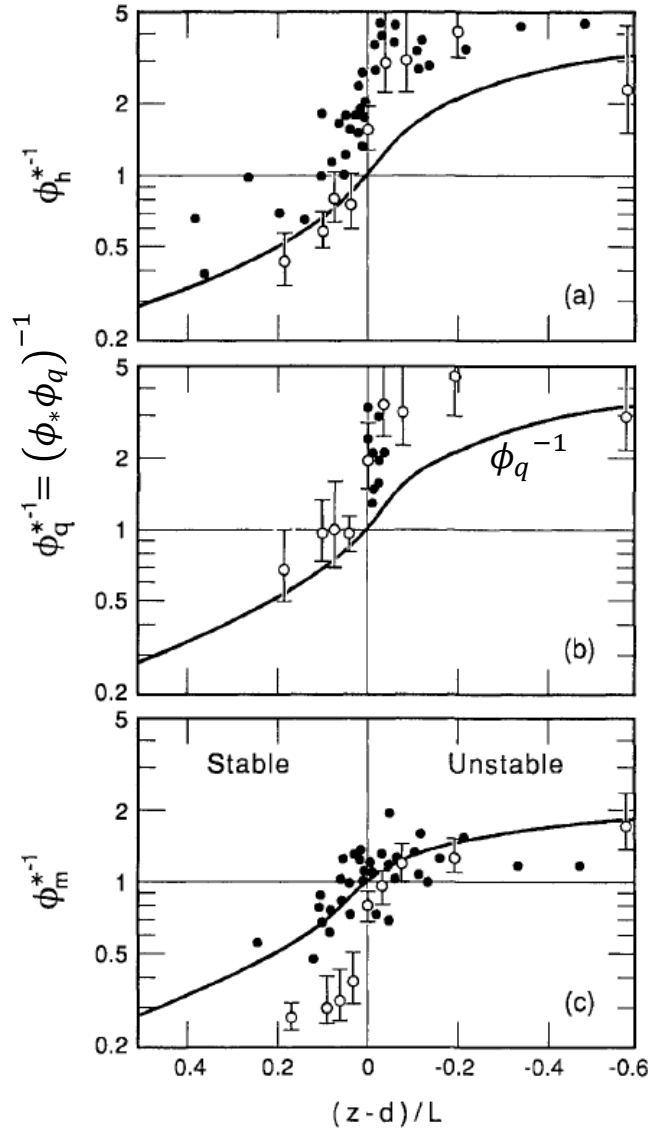

Flow within the Canopy

$$u(z) = u(h_c)\exp\left(\alpha\left(\frac{z}{h_c} - 1\right)\right)$$

α is an extinction coefficient, a function of leaf-area-index (LAI), canopy height (h_c), leaf separation (l_m):

$$\alpha = \frac{0.2\ \mathrm{LAI}\ h_c}{l_m}$$

Table 3.5. Values of the profile parameter of the wind profile within the plant canopy in Eq. (3.10) according to Cionco (1978)

plant canopy	profile parameter α
wheat	2.45
rye	1.97
rice	1.62
sun flowers	1.32
larch tree plantation	1.00
fruit plantation	0.44

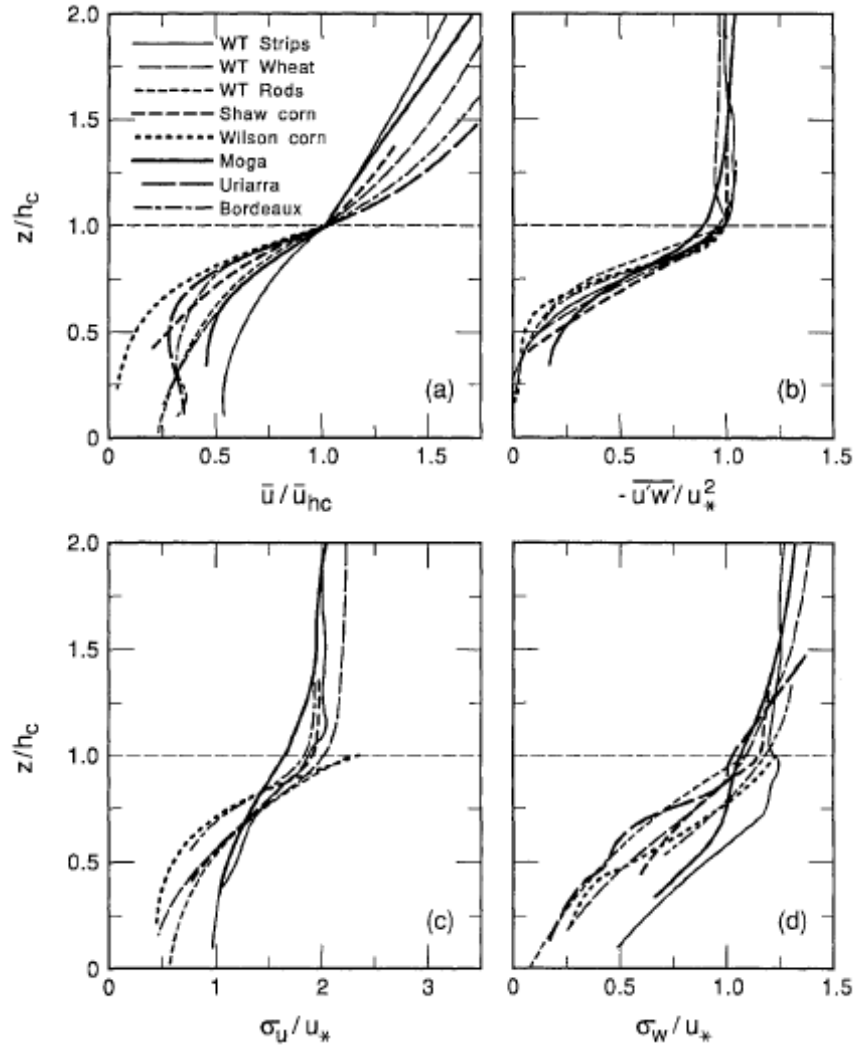

Foken, Ch 3. Kaimal & Finnigan, Ch 3

Momentum Balance

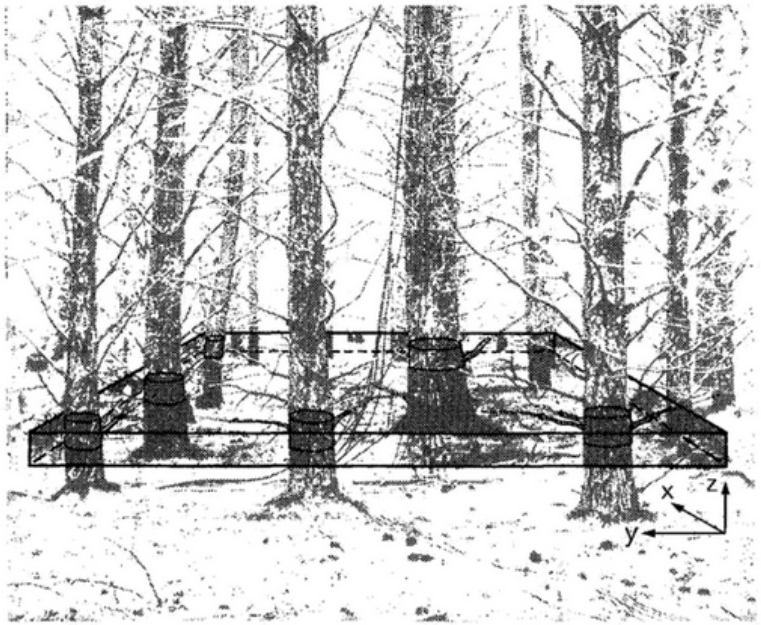

Fig. 3.7. Schematic view of an averaging volume V in a forest. The solid plant parts are excluded from the average, causing V to be a "multiply connected" space.

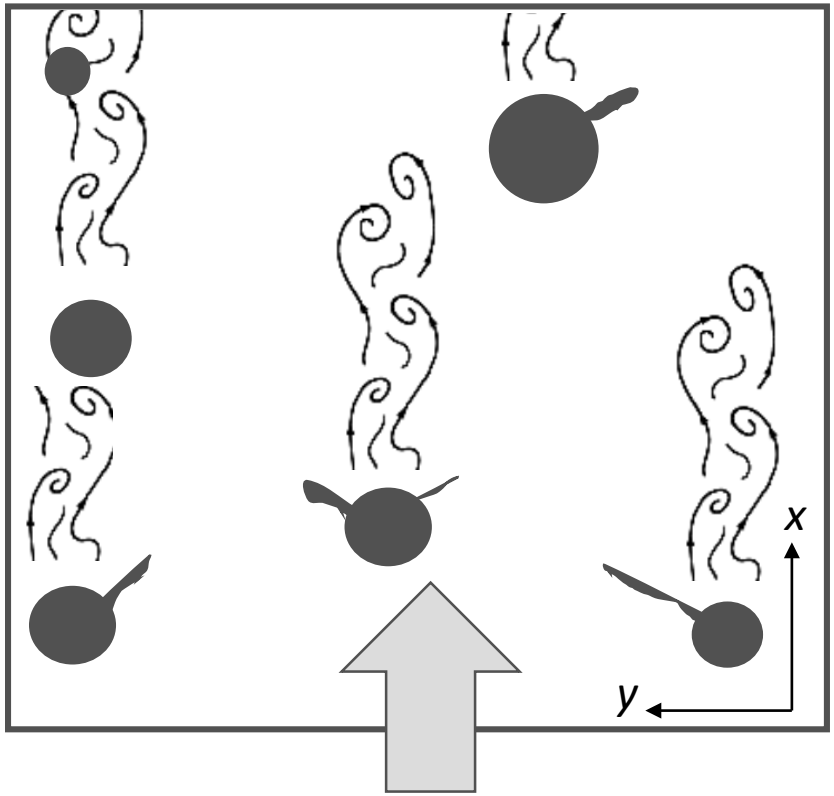

Drag forces from the canopy elements disrupt the random nature of the turbulence and lead to the failure of simple K-Theory.

Kaimal and Finnigan, 1994, Atmospheric Boundary Layer Flows. Oxford

Momentum Balance

$$\frac{D}{Dt}\langle\overline{u}\rangle = 0 = -\frac{\partial}{\partial z}\langle\overline{u'w'}\rangle - \frac{\partial}{\partial z}\langle\overline{u}''\overline{w}''\rangle - \frac{\langle\overline{D}\rangle(z)}{\rho},$$

$\langle u'w'\rangle$ Shear stress.

$\langle u''w''\rangle$ Dispersive flux of momentum (<1% shear stress).

$\langle D\rangle$ Canopy drag.

$$u_*^2 \neq K\frac{du}{dz}$$

Kaimal and Finnigan, 1994, Atmospheric Boundary Layer Flows. Oxford

Near-Field Theory

Canopy Diffusion:

$$K_f = R\left(\frac{\tau}{T_L}\right)K_z$$

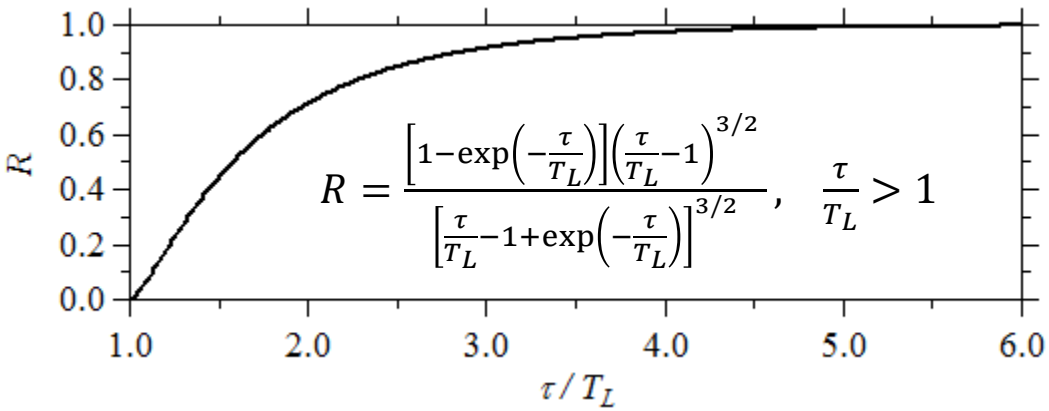

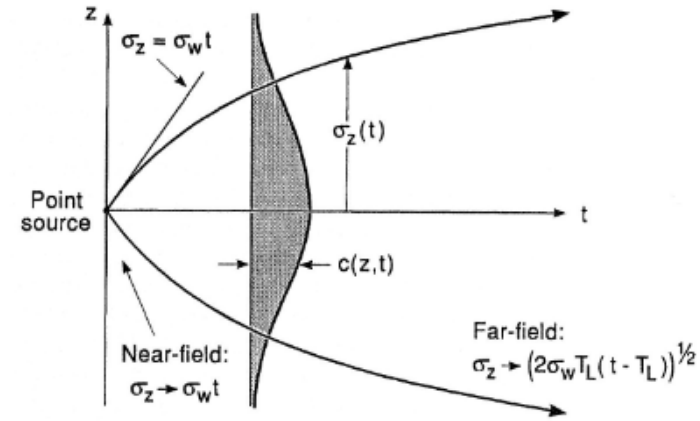

Fig. 3.10. Kaimal and Finnigan, Atmospheric Boundary Layer Flows

τ is a transport lifetime

T_L is the Lagrangian timescale, loosely defined as:

"The persistence of turbulent eddies or the memory of the flow."

Raupach, 1989, A practical Lagrangian method for relating scalar concentrations to source distributions in vegetation canopies. Q.J.R. Meteorol. Soc.

Vertical Temperature Structure

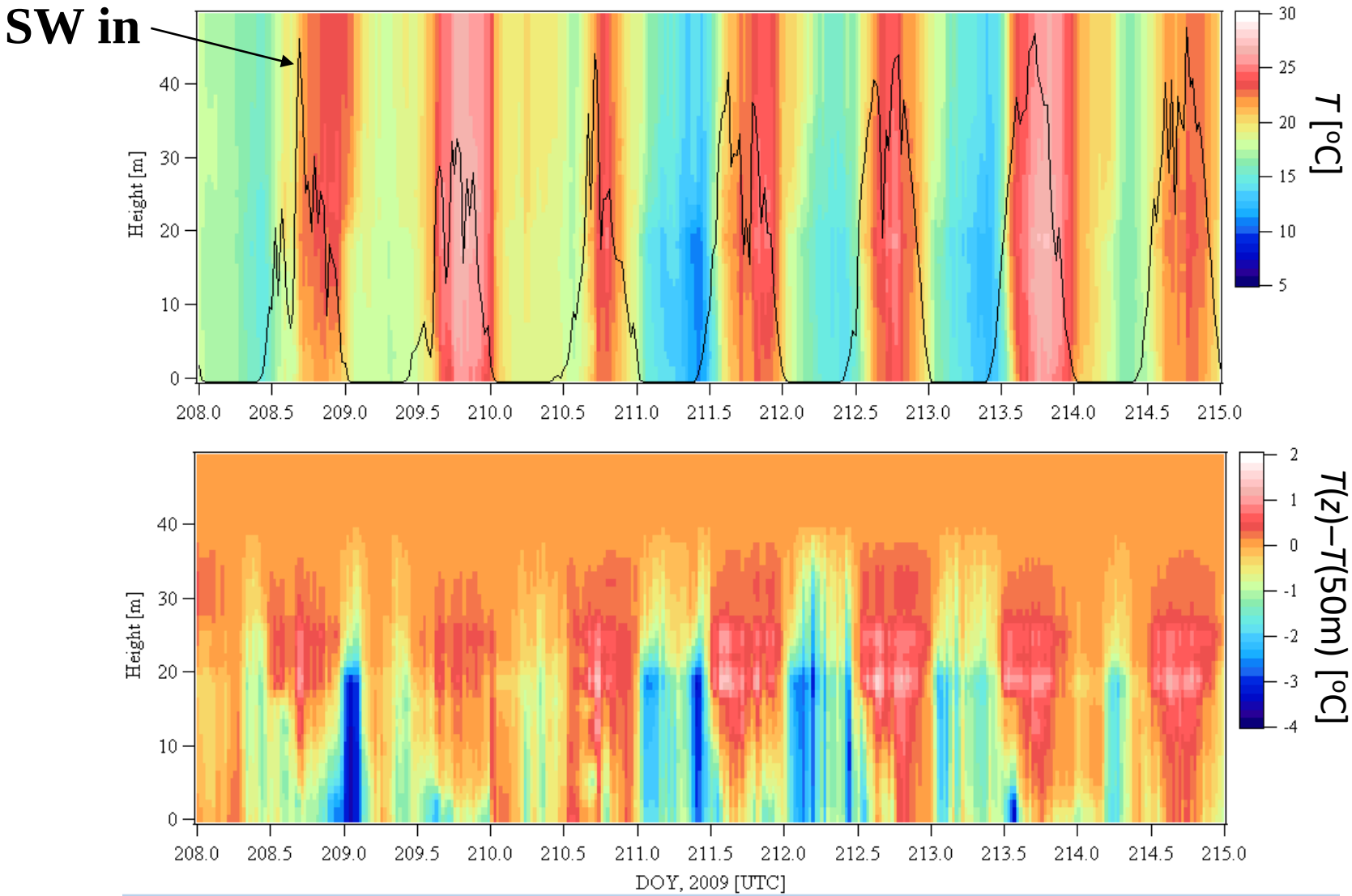

Counter-Gradient Turbulence

$$H = \overline{w'T'} \qquad \lambda E = \overline{w'q'}, \qquad F = \overline{w'c'}$$

$$\neq -K_z \frac{dT}{dz} \qquad \neq -K_z \frac{dq}{dz} \qquad \neq -K_z \frac{d\rho}{dz}$$

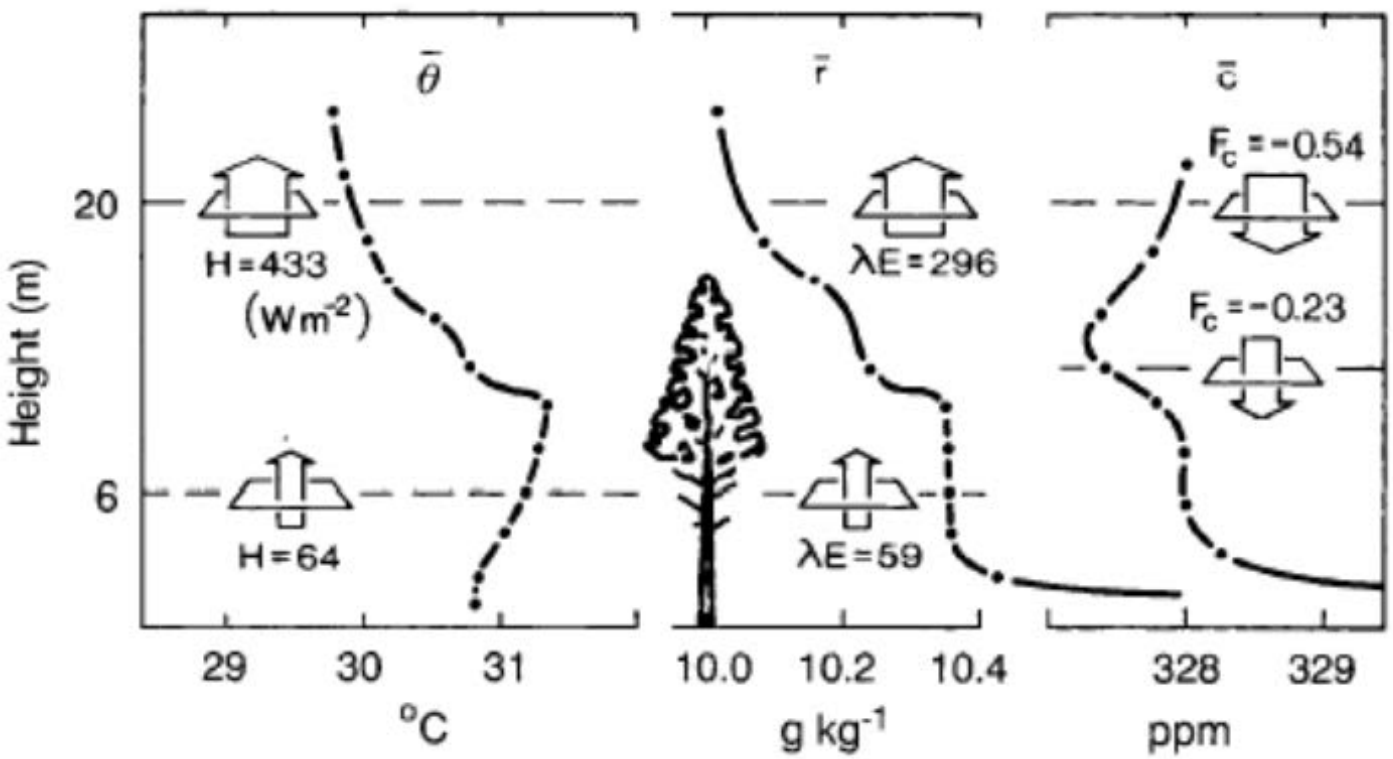

Fig. 2. Simultaneous fluxes and gradients of heat and temperature, latent heat and water vapour mixing ratio and carbon dioxide. Obtained in a pine forest. Figure from Denmead and Bradley, 1985.

Kaimal and Finnigan, 1994, Atmospheric Boundary Layer Flows. Oxford

Turbulent Structures

"Coherent structures, in contrast to stochastically distributed turbulence eddies, are well organized, relatively stable long-living eddy structures, which occur mostly with regularity in either time or space."*

**

u
[m/s]

ΔT
[°C]

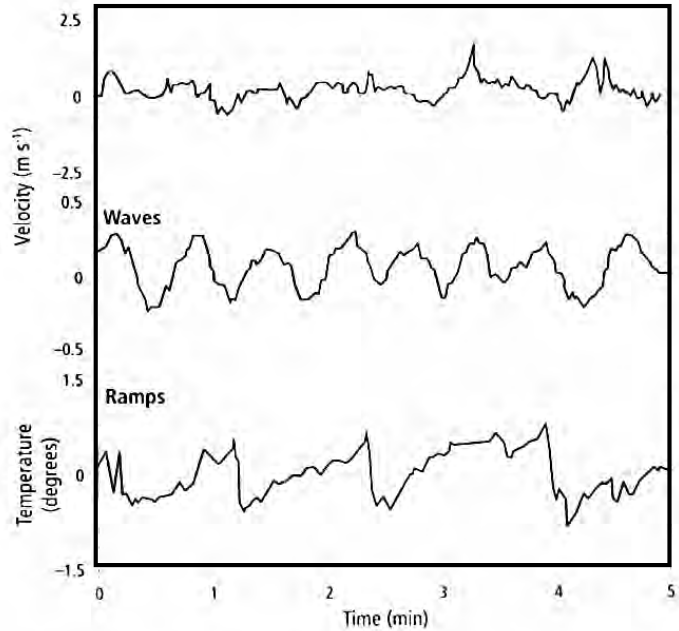

Fig. 3.25. Fluctuations, waves and ramp structures above a forest (Bailey *et al.* 1997) by using data from Gao *et al.* (1989) and Amiro and Johnson (1991) **

* Holmes et al. 1996, Turbulence, coherent structures, dynamical systems and symmetry. Cambridge
** Foken, 2008, Micrometeorology. Springer

Coherent Structures

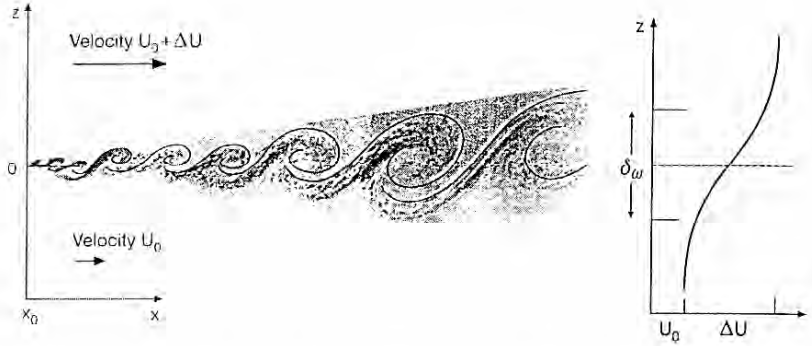

Fig. 3.28. Developing of the mixing layer of the height δ_w (Raupach *et al.* 1996)

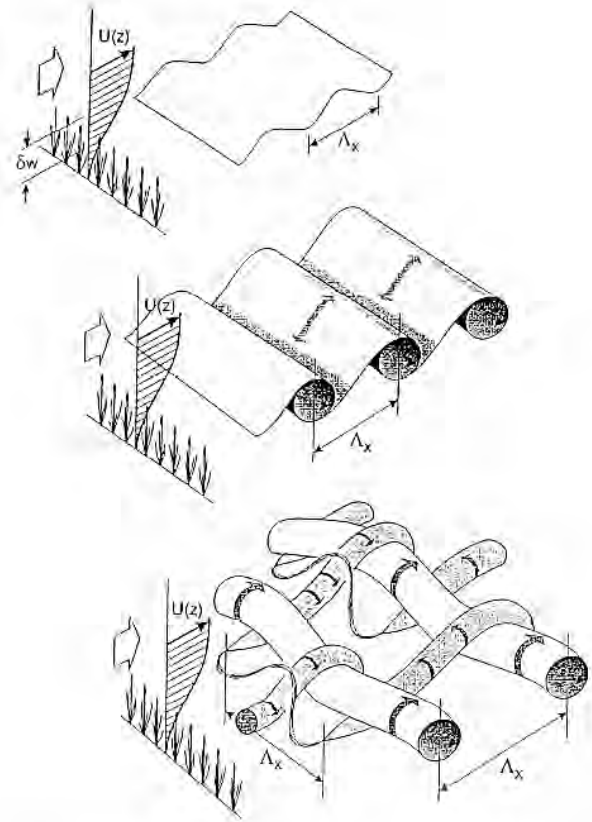

Fig. 3.29. Schematic description of the developing of the mixing layer above a plant canopy (Finnigan 2000)

Foken, 2008, Micrometeorology. Springer

Eddy Covariance (+'ve)

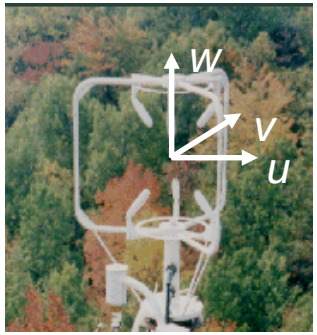

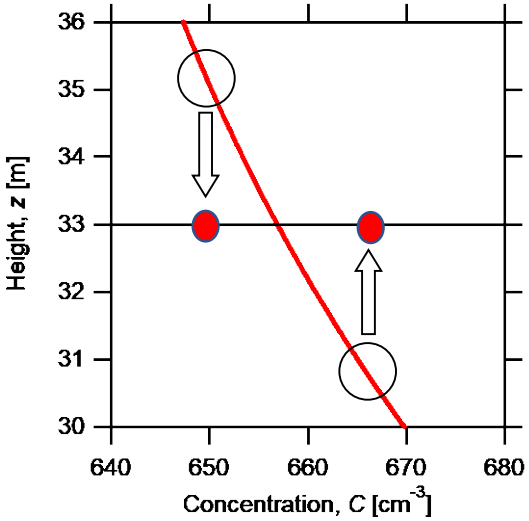

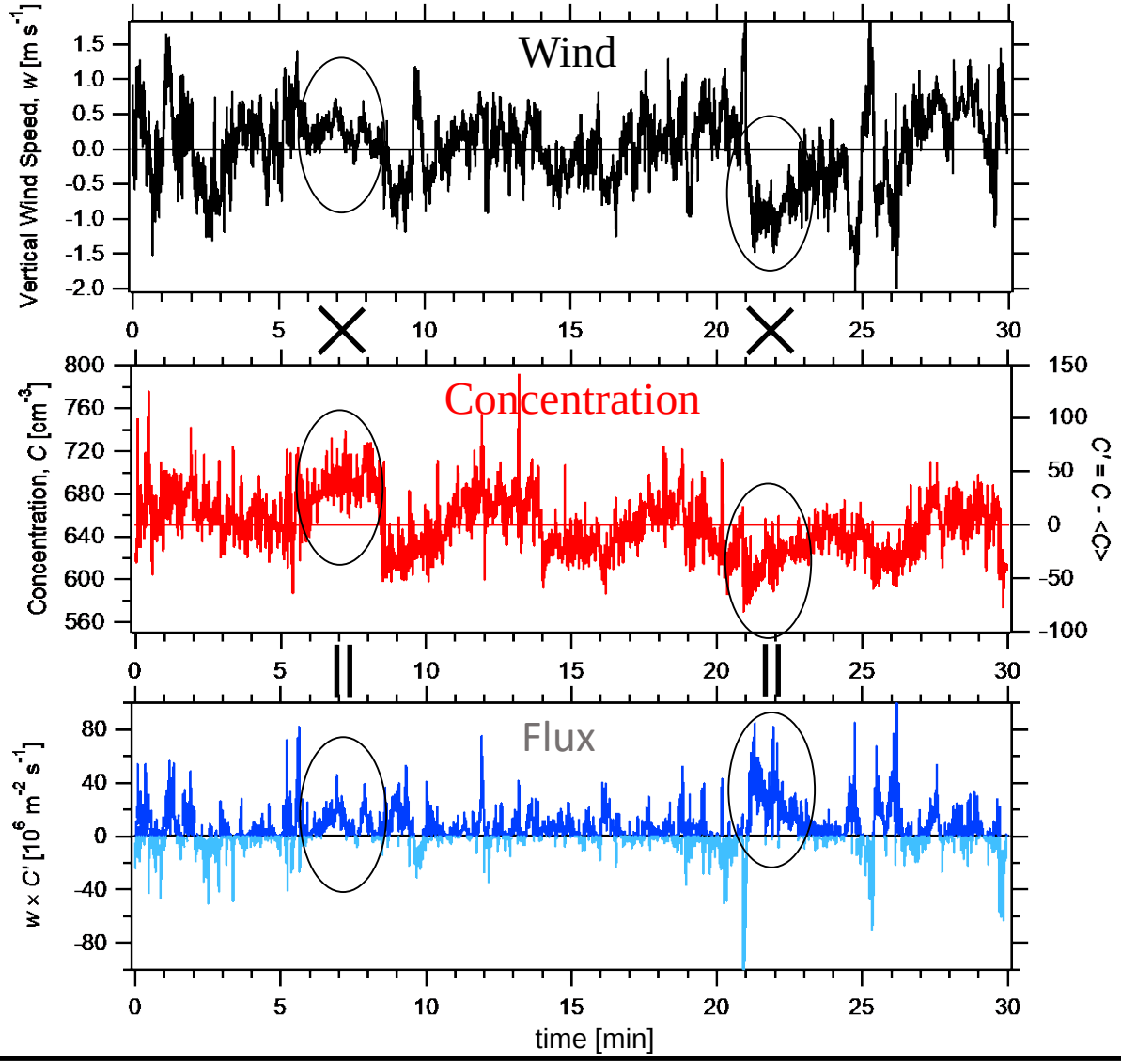

Eddy Covariance (–'ve)

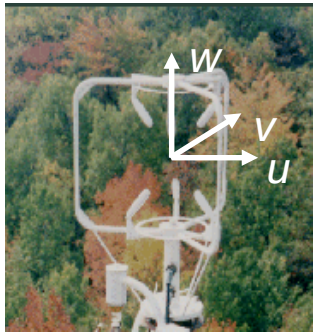

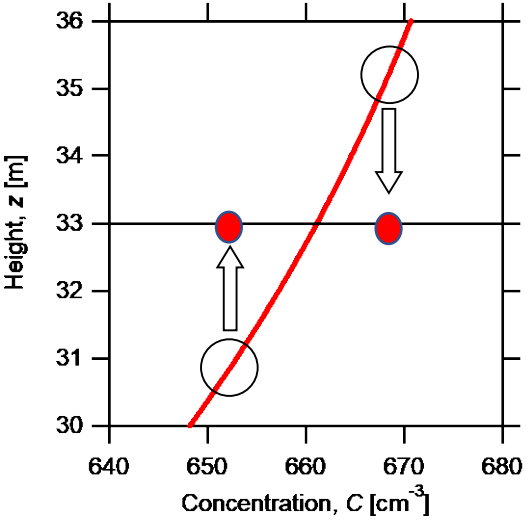

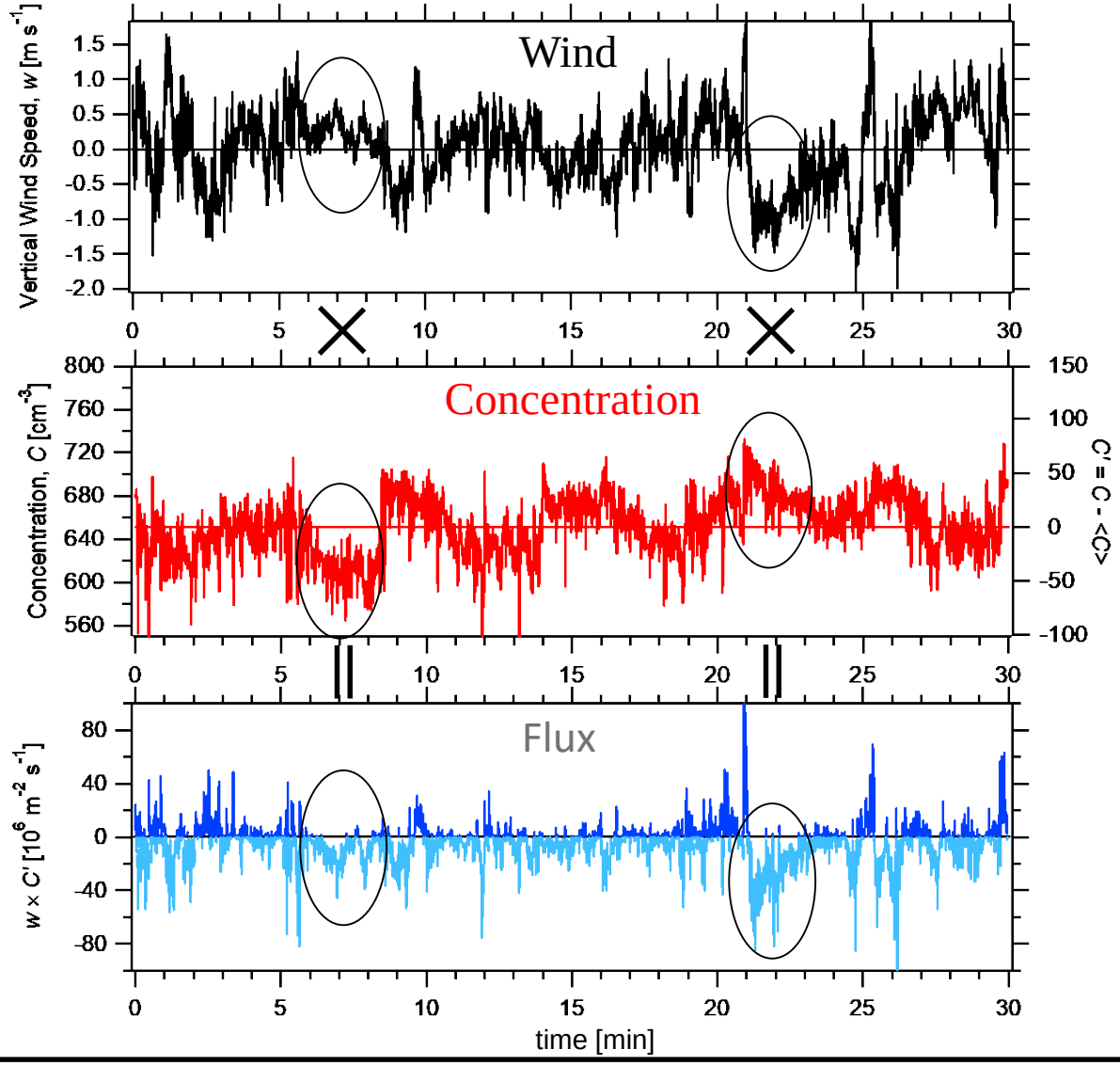

Bursts and Sweeps

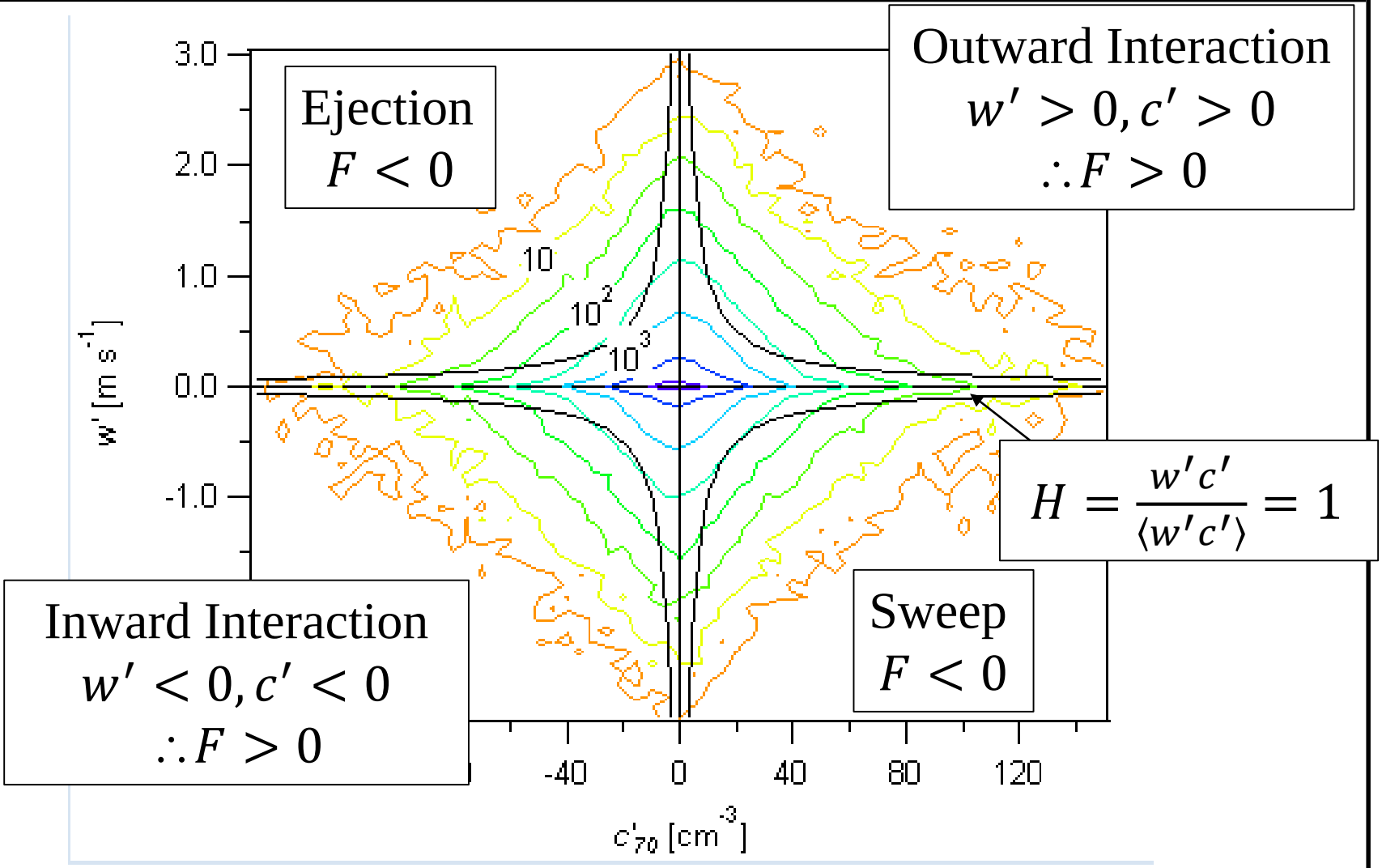

70 um Aerosol concentration measured at 33 m height at Borden Forest.

Bursts and Sweeps

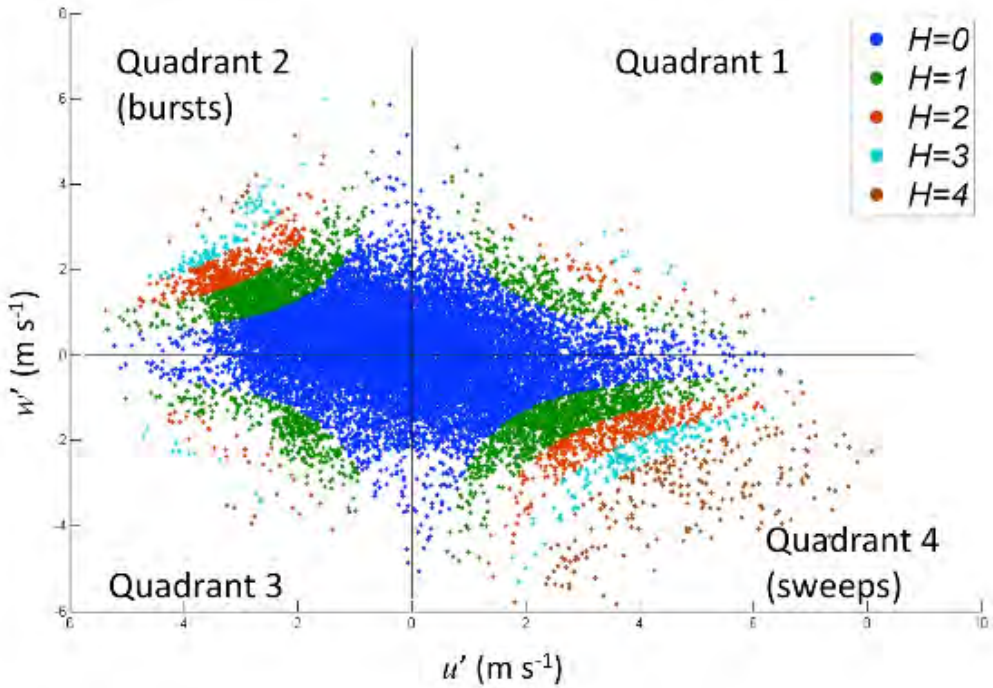

$$H = \frac{u'w'}{\langle u'w' \rangle}$$

Fig. 2. Sample 30-min analysis (28 July (DOY 209), 12:30–13:00 LT) using the quadrant analysis method for different hole sizes. Each point represents a 10 Hz sonic data point. Note as the hole size increases weak events are excluded, thus for large hole sizes ($H = 4$) only extreme events are considered.

Steiner et al., 2011, Analysis of coherent structures and atmosphere-canopy coupling strength during the CABINEX field campaign. *ACP*

Schematics of Canopy Mixing

Table 3.9. Characterization of the states of coupling between the atmosphere and tall plant canopies (Thomas and Foken 2007b). The signature with letter is according to the coupling stages in Fig. 3.30 (Figures from Göckede *et al.* 2007)

Wa	Dc	Ds	Cs	C
				
gravity waves above the canopy	turbulent eddies only above the canopy	turbulent mixing up to the crown	occasionally complete mixing of the canopy	complete mixing of the canopy
no coupling	no coupling	occasionally weak coupling	occasionally coupling	good coupling

Foken, 2008, Micrometeorology. Springer

Schematics of Canopy Mixing

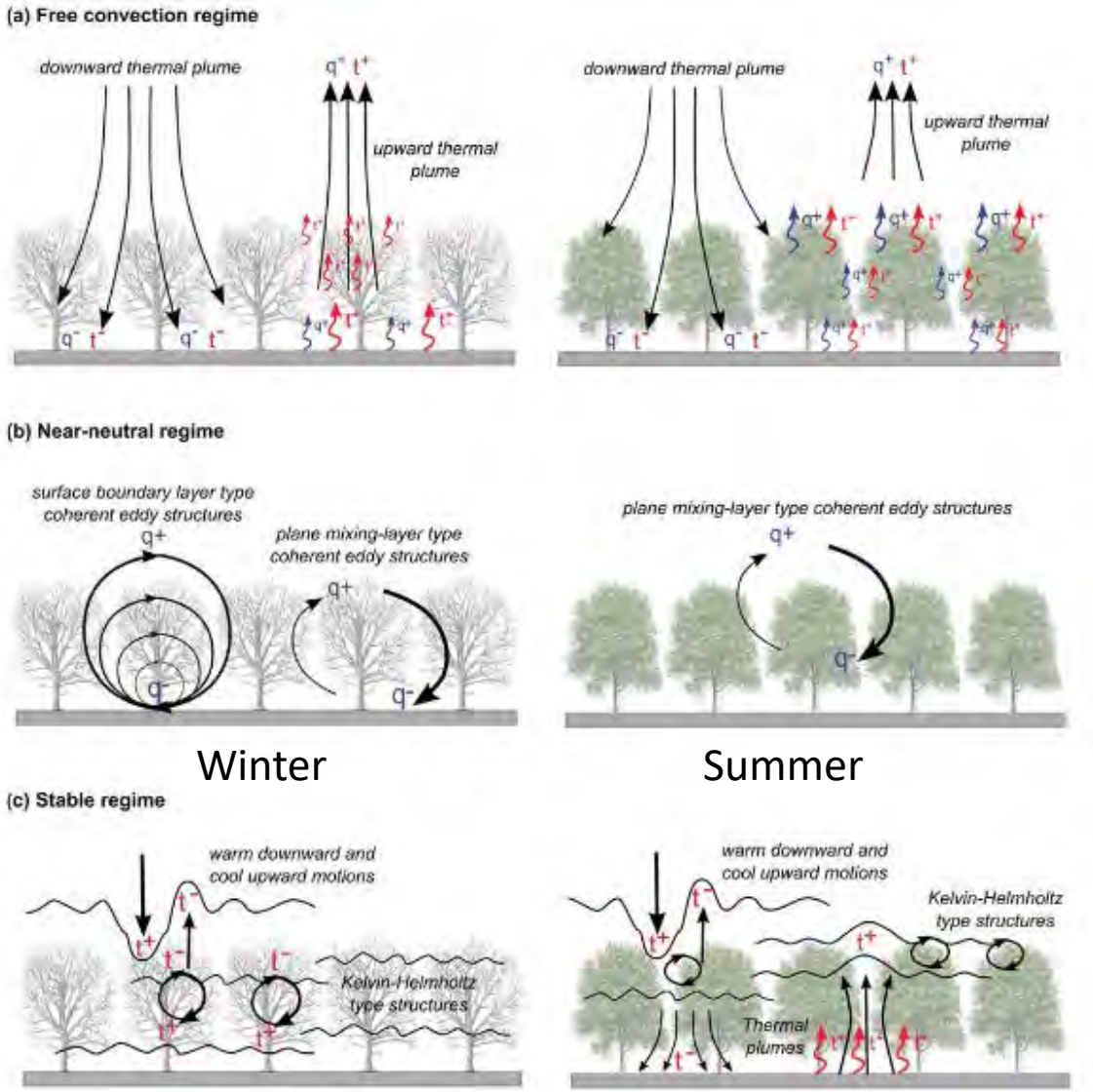

Fig. 12. Idealized representation of the turbulent structures transporting momentum and scalars (temperature *t* and water vapor *q*) at CHATS and their main characteristics during: (a) free convection, (b) near-neutral, and (c) stable regimes for both seasonal periods (without and with leaves).

Dupont & Patton: Stability and seasonal influences on canopy transport, *ACP*.

The Profile Flux Method

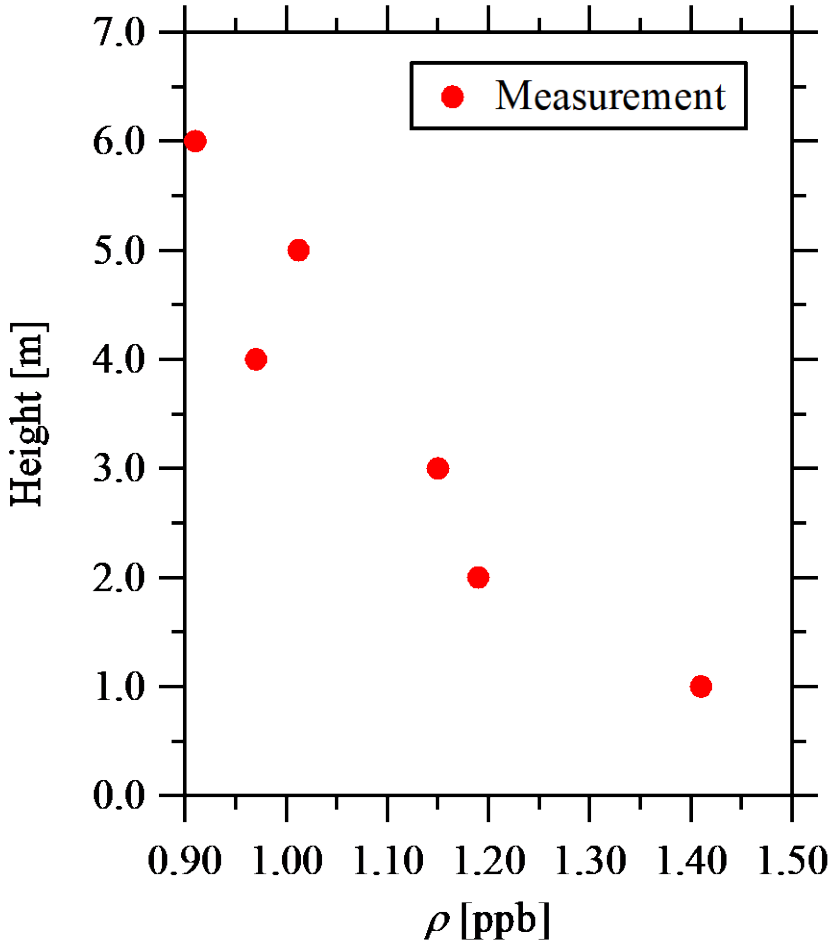

$$F = -K\frac{d\rho}{dz} \qquad K = \kappa\, u_* z/\phi$$

F : Flux [kg m^{-2} s^{-1}]

K : Diffusion Coefficient [m^2 s^{-1}]

$\frac{d\rho}{dz}$: Concentration Gradient [kg m^{-3} m^{-1}]

κ = 0.4

u_* : Friction Velocity [m s^{-1}]

z : Height [m]

ϕ : Stability Parameter

The Profile Method

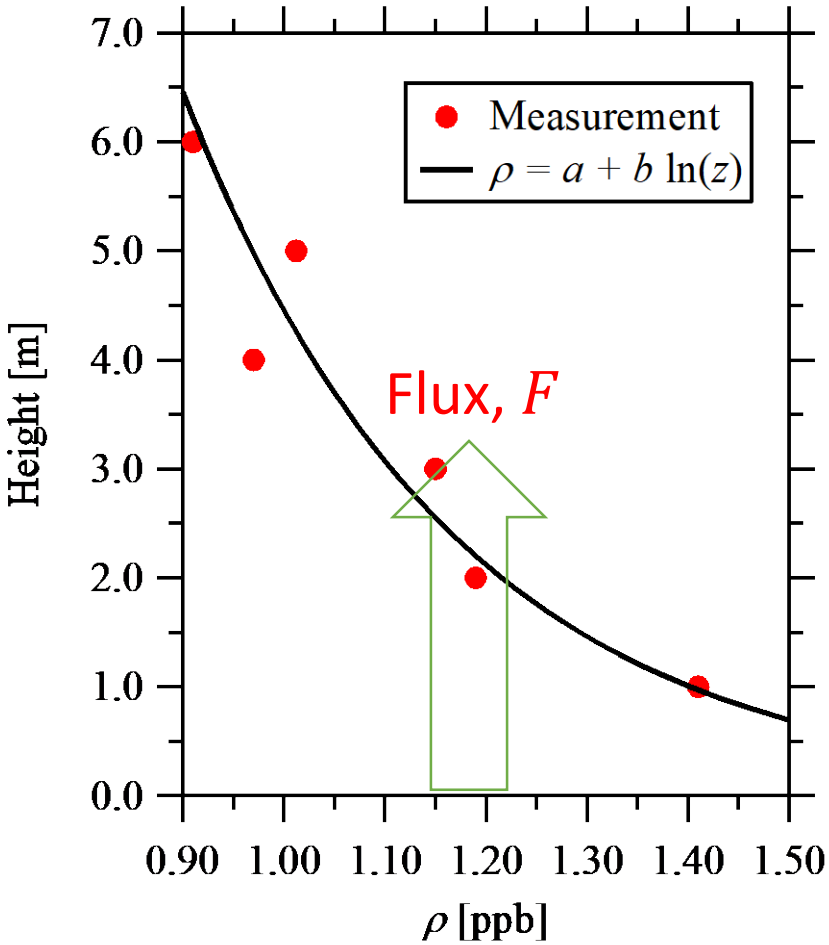

$$F = -K\frac{d\rho}{dz} \qquad K = \kappa\, u_* z/\phi$$

$$\rho(z) = \rho(z_r) - \frac{F}{\kappa\, u_*/\phi}\ln\left(\frac{z}{z_r}\right)$$

Best fit: $\rho(z) = \rho(z_r) + b\ln\left(\frac{z}{z_r}\right)$

Flux, $F = -b\kappa\, u_*/\phi$

Inverse Lagrangian Method

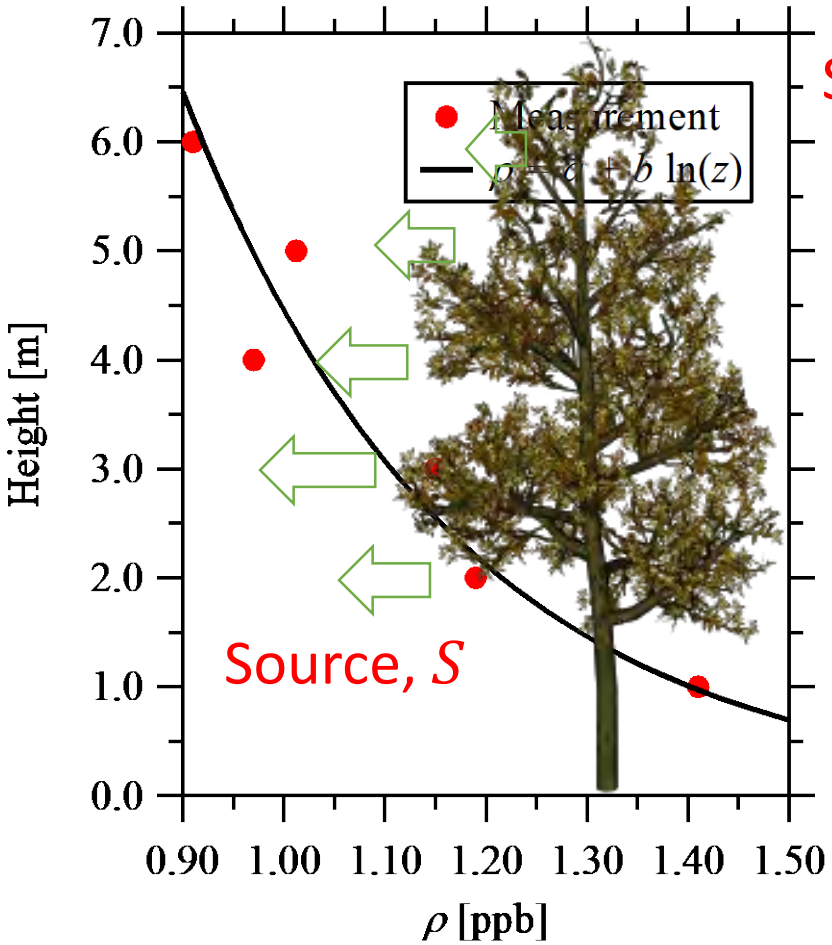

Source ⇨ $\int \bar{S}\, dz = -K \dfrac{d\rho}{dz}$ ⇦ Flux

$$\left.\frac{d\rho}{dz}\right|_i = \sum_{j=1}^{m} M_{ij}\, S_j\, \Delta z_j$$

The inverse mixing matrix (M_{ij}^{-1}) is analogous to the diffusion coefficient K.

It is parameterized and the source function (S_i) is solved through an optimization procedure.

Warland JS, Thurtell G (2000) Boundary-Layer Meteorol 96(3): 453–471

Profile Measurements

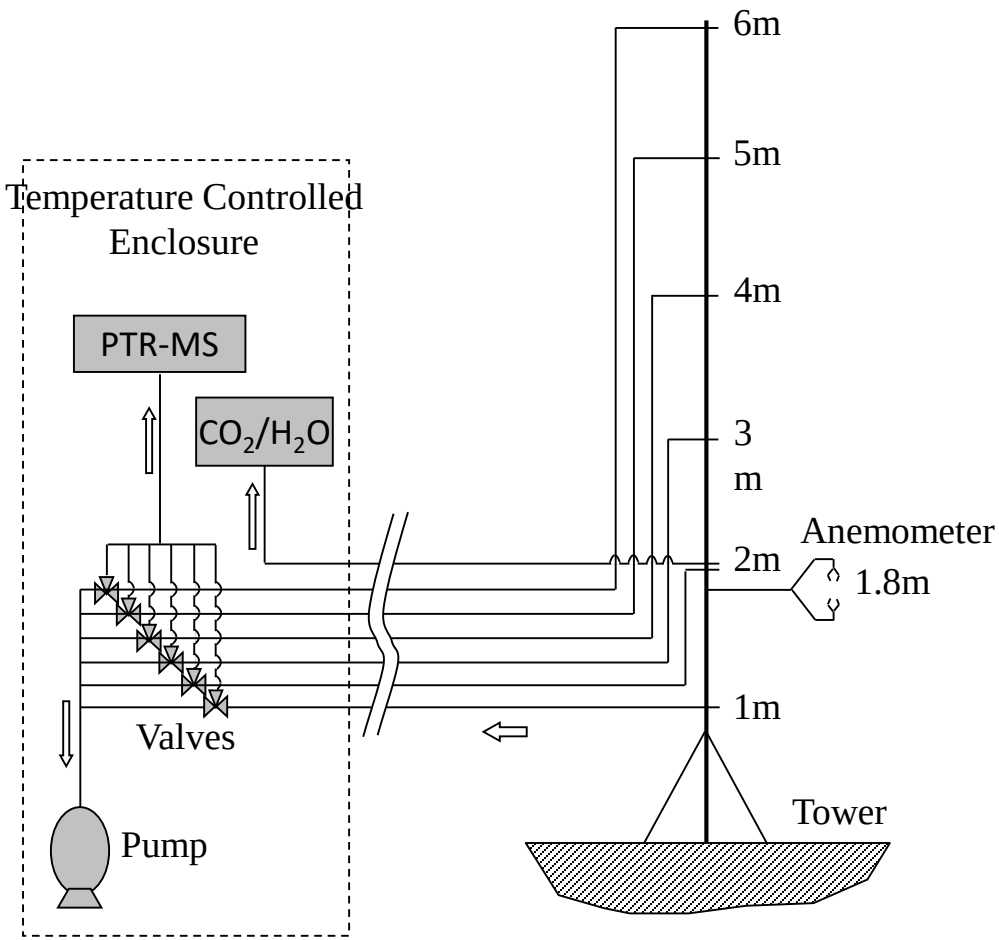

Latent Hear Fluxes (EC, Profile, ILM)

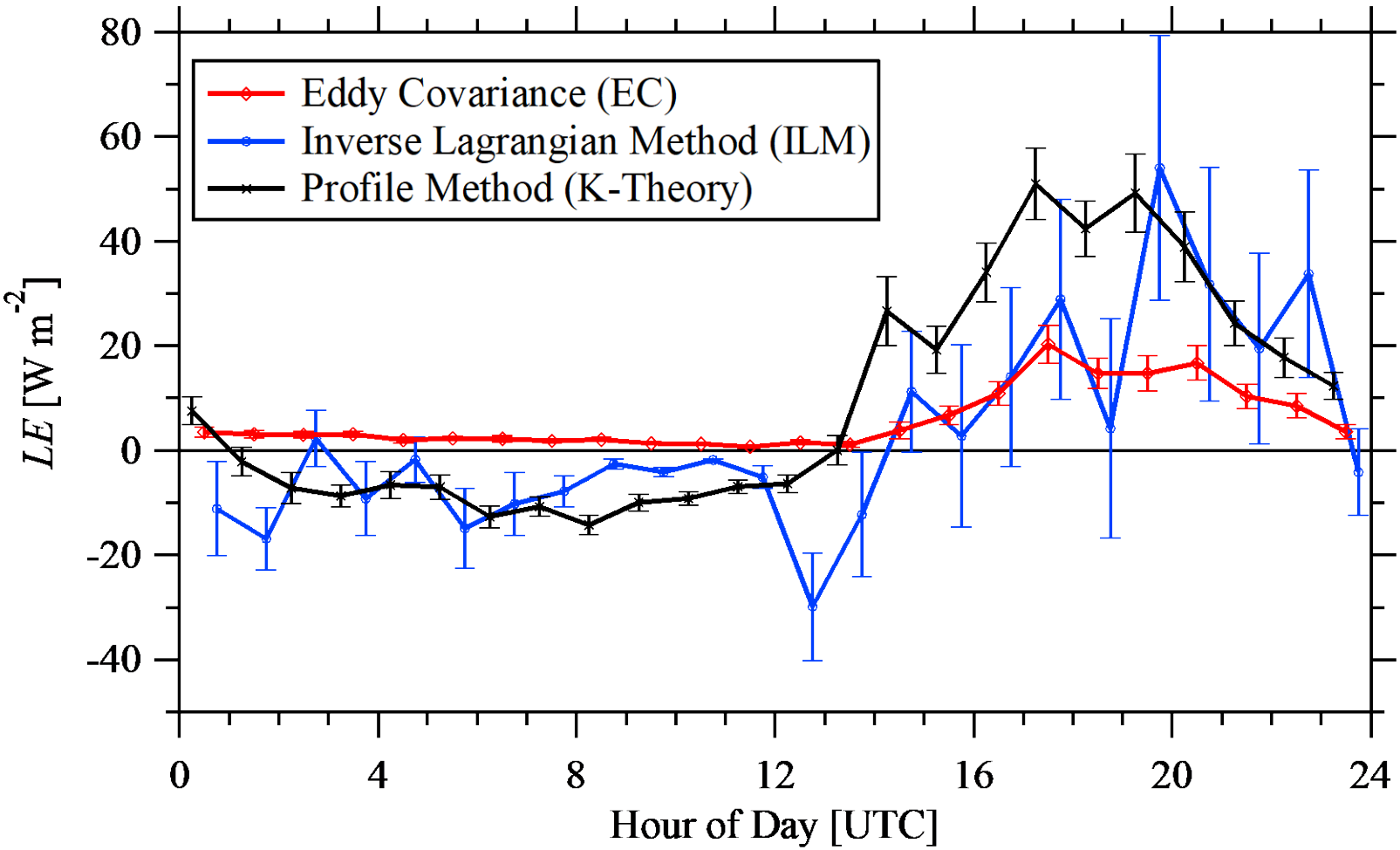

Gordon et al. (2014) ACP, 14, 9087–9097

Decoupling of the Canopy Space

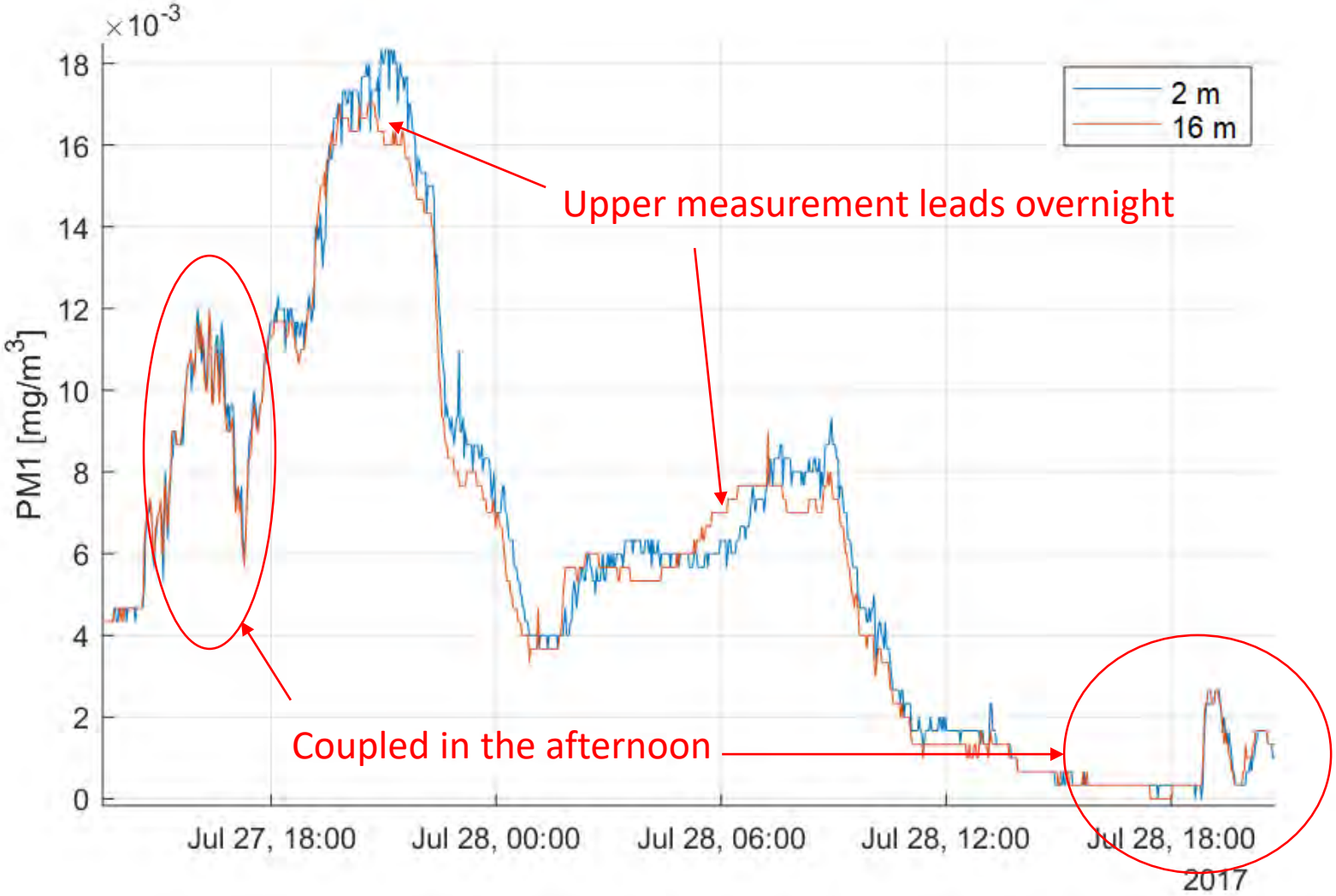

Jiang (2018) MSc Thesis, York

Decoupling of the Canopy Space

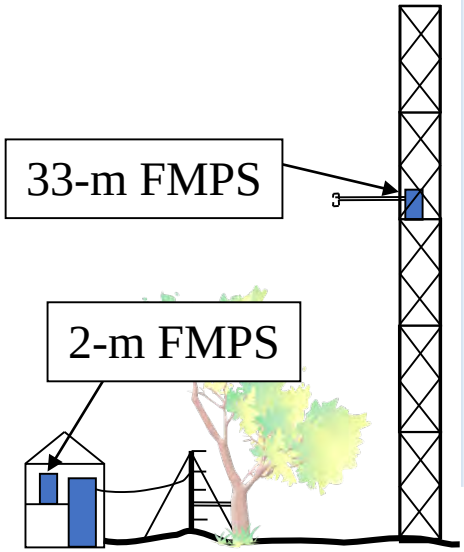

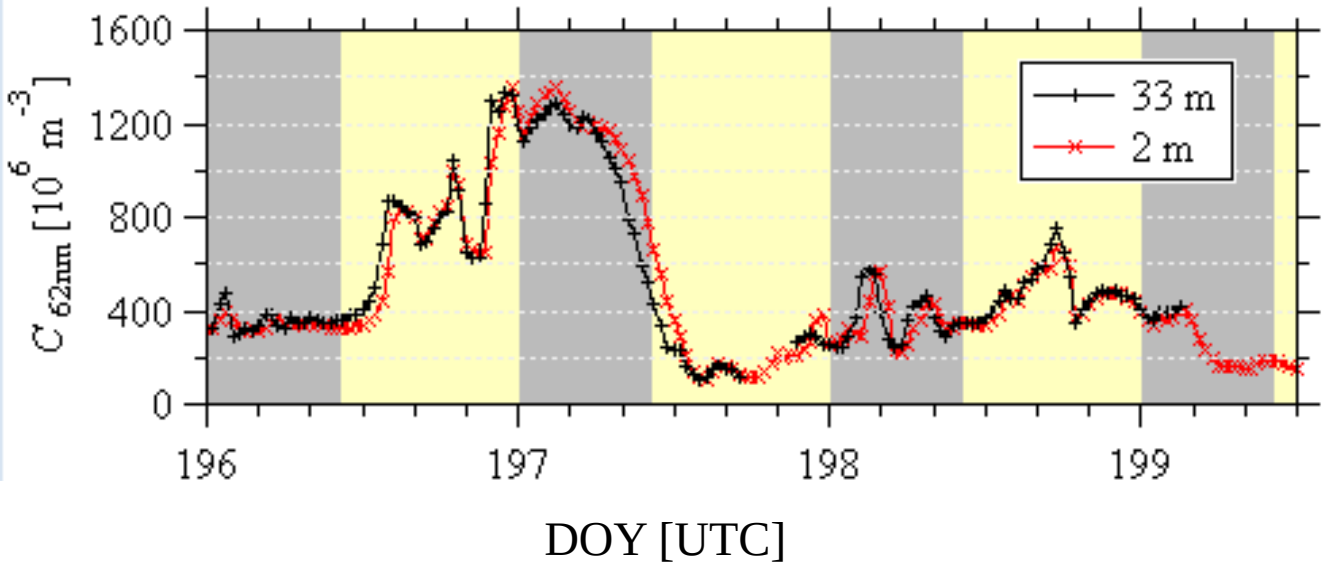

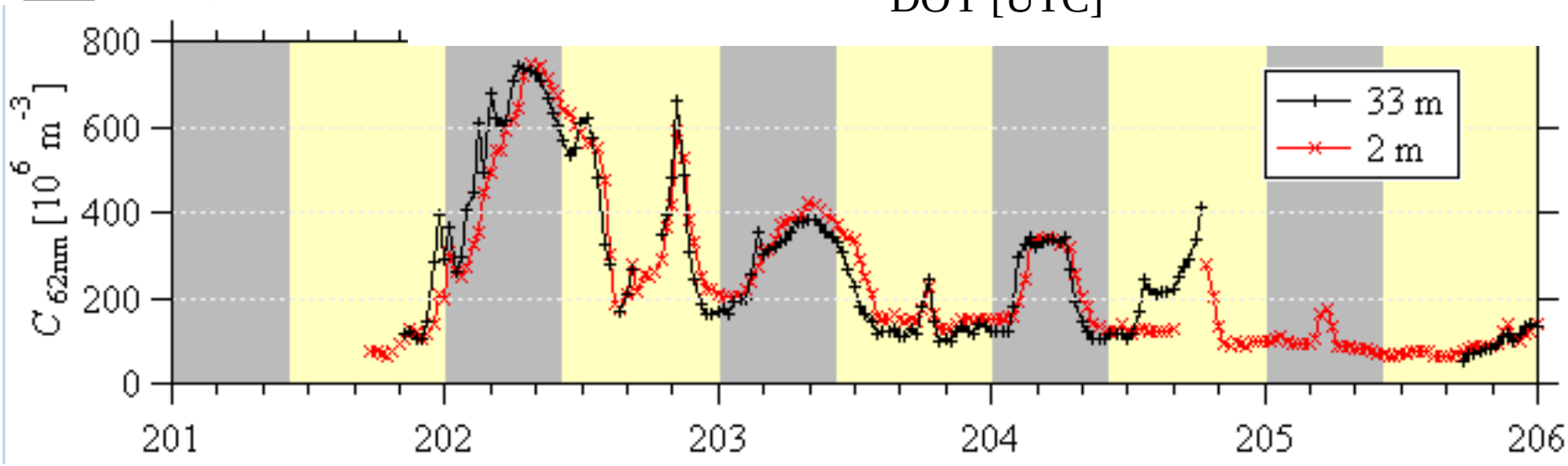

Gordon et al. (2011) ACP, 11, 11, 6773–6786

Delay Time of Decoupling

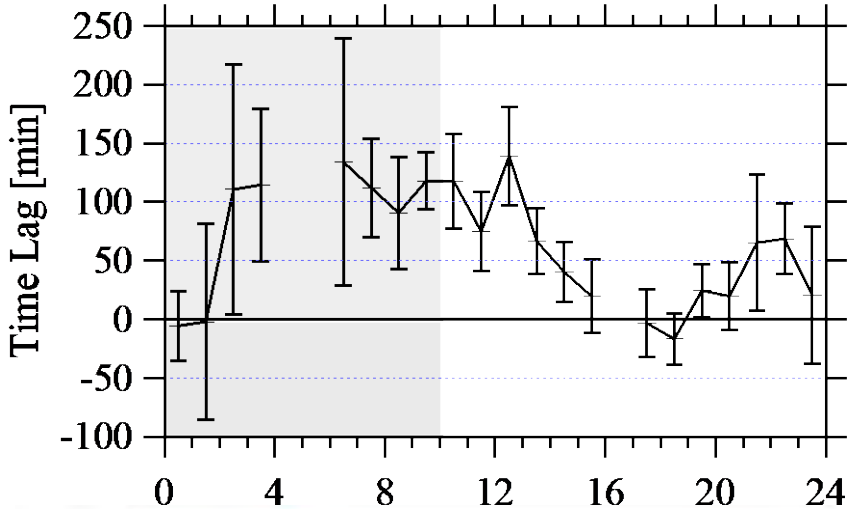

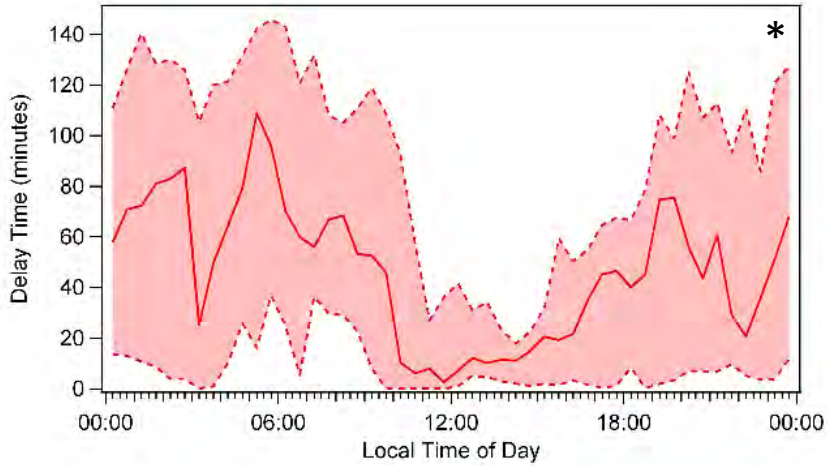

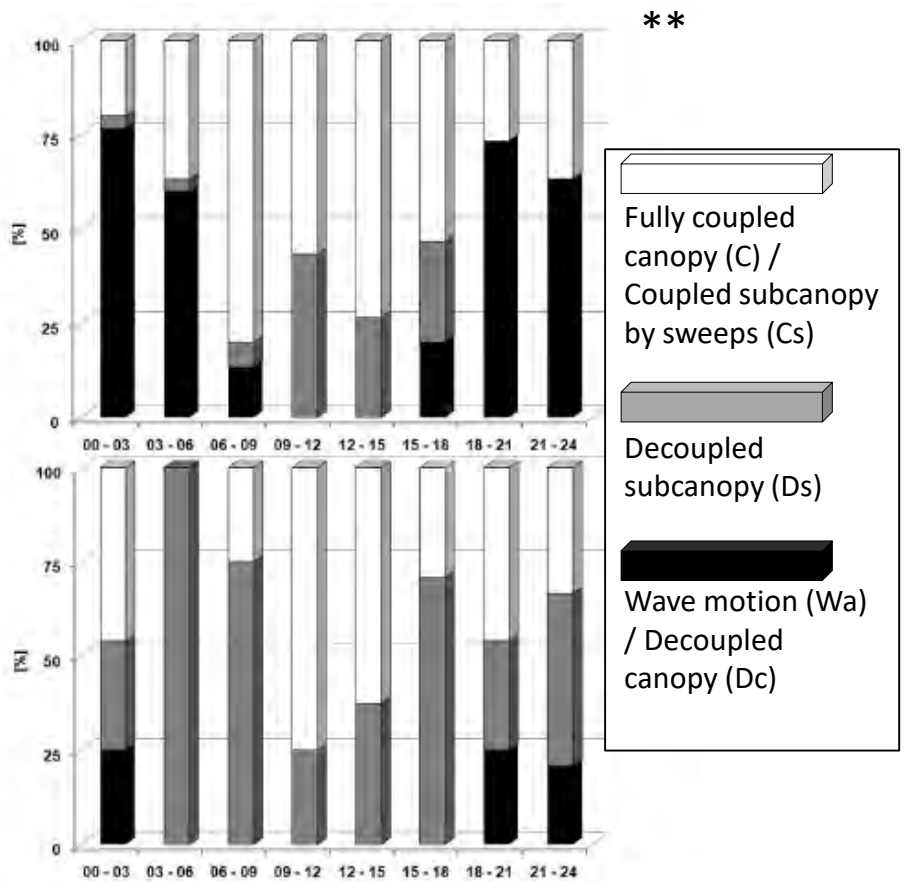

Fig. 4. Percentage of different coupling classes during the Golden Days of IOP-1 (left, 30 three-hour periods) and IOP-2 (right, 24 three-hour periods) in the daily cycle.

*Whitehead et al., 2010, Aerosol fluxes and dynamics…tropical rainforest in South-East Asia. *ACP*

**Foken et al., 2012, Coupling processes and exchange of energy… EGER experiment. *ACP*